Available online at www.sciencedirect.com
ScienceDirect
Ceramics International 37 (2011) 1979–1983
CERAMICS INTERNATIONAL
www.elsevier.com/locate/ceramint

Microstructures and dielectric properties of spark plasma sintered $Ba_{0.4}Sr_{0.6}TiO_3/CaCu_3Ti_4O_{12}$ composite ceramics

Y.J. Wu *, S.H. Su, S.Y. Wu, X.M. Chen

Laboratory of Dielectric Materials, Department of Materials Science and Engineering, Zhejiang University, Zheda Road 38, Hangzhou 310027, China

Received 13 January 2011; received in revised form 9 February 2011; accepted 11 February 2011
Available online 19 February 2011

Abstract

$(1-x)Ba_{0.4}Sr_{0.6}TiO_3/xCaCu_3Ti_4O_{12}$ composite ceramics were prepared by spark plasma sintering. Sintering behavior, microstructures and dielectric properties of the composite ceramics were investigated by XRD, SEM, EDS and dielectric spectrometer. Dense composite ceramics consisting of $Ba_{0.4}Sr_{0.6}TiO_3$ phase and $CaCu_3Ti_4O_{12}$ phase were prepared at 800 °C for 0 min. The dielectric loss of the composite ceramic decreased with increasing amount of $Ba_{0.4}Sr_{0.6}TiO_3$, and the high dielectric constant were retained. Moreover, the better temperature stability of dielectric constant was obtained. These improvements of dielectric characteristics have great scientific significance for potential application.

Keywords: A. Sintering; B. Composites; C. Dielectric properties; D. $BaTiO_3$ and titanates

1. Introduction

The miniaturization of electronic devices has increased the demand of dielectric ceramics with high dielectric constant, low dielectric loss and good temperature stability. Recently, $CaCu_3Ti_4O_{12}$ (CCTO) with complex perovskite structure has attracted much scientific attention because of its giant dielectric constant over a wide range of temperature and frequency [1–4]. However, pure CCTO have difficulties in satisfying the requirements of potential application due to its high dielectric loss and relatively large temperature dependence of dielectric constant. One promising method to overcome these problems is to prepare composite ceramics of CCTO and other oxides with low dielectric loss [5–9]. $BaTiO_3$–$CaCu_3Ti_4O_{12}$ (BTO–CCTO) composite with low dielectric loss has been prepared by Fechine et al. [5]. Yang et al. fabricated $(1-x)BaTiO_3$–$xCaCu_{2.94}Mn_{0.06}Ti_4O_{12}$ (BTO–CCMTO) composite with low dielectric loss by a traditional solid-state method [6]. Compared with BTO, $Ba_{1-x}Sr_xTiO_3$ (BST) with a lower Curie temperature offers another advantage for modification of the temperature dependence of dielectric constant of CCTO [10–12].

On the other hand, spark plasma sintering (SPS) has been widely investigated as a rapid preparation method to prepare composite materials [13–16]. It is a newly developed sintering technology that makes use of microscopic electrical discharges between particles under pressure and allows for quick densification [17–23]. In addition, a relatively low sintering temperature and a short sintering time are the most attractive features for preparing multi-phase materials [13–16].

In this paper, $Ba_{0.4}Sr_{0.6}TiO_3/CaCu_3Ti_4O_{12}$ (BST/CCTO) composite ceramics were prepared by spark plasma sintering. The sintering behavior, microstructures and dielectric properties of the composite ceramics were investigated.

2. Experimental

$Ba_{0.4}Sr_{0.6}TiO_3$ and $CaCu_3Ti_4O_{12}$ powders were synthesized via a standard solid state reaction method, respectively. Stoichiometric mixture of $SrCO_3$ (>99.9%), $BaCO_3$ (>99.93%) and TiO_2 (>99.5%) were well ground and calcined at 1150 °C in air for 3 h to yield $Ba_{0.4}Sr_{0.6}TiO_3$. Meanwhile, well-ground stoichiometric mixture of $CaCO_3$ (>99.99%), CuO (>99%) and TiO_2 (>99.5%) were heated to 1025 °C in air for 3 h to prepare $CaCu_3Ti_4O_{12}$. The mixture of $(1-x)Ba_{0.4}Sr_{0.6}TiO_3/xCaCu_3Ti_4O_{12}$ with $x = 0.3$, 0.5 was re-milled, placed in a graphite die, and sintered at 800 °C under a vacuum of 6 Pa with

* Corresponding author. Tel.: +86 57187951410; fax: +86 57187951410.
E-mail address: yongjunwu@zju.edu.cn (Y.J. Wu).

0272-8842/$36.00
doi:10.1016/j.ceramint.2011.02.006

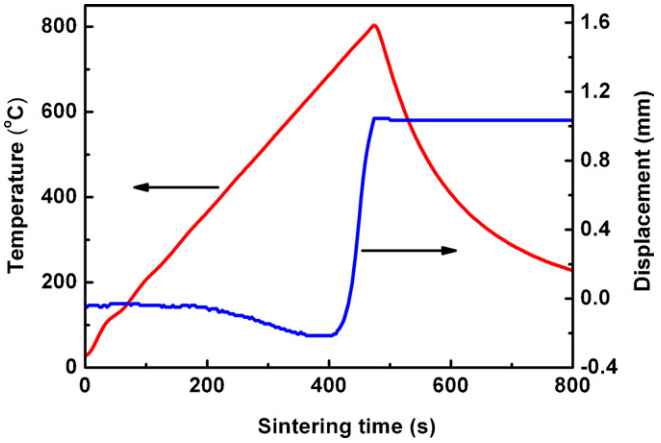

Fig. 1. Shrinkage curve and sample's temperature as a function of sintering time in spark plasma sintering of 0.7BST/0.3CCTO composite ceramics.

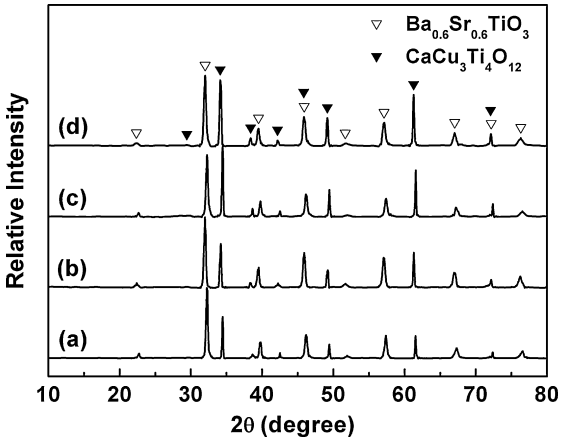

Fig. 2. X-ray diffraction patterns of $(1-x)$BST/xCCTO composite ceramics. (a) $x = 0.3$, spark plasma sintered at 800 °C; (b) $x = 0.3$, subsequently heat treated at 600 °C for 2 h; (c) $x = 0.5$, spark plasma sintered at 800 °C; (d) $x = 0.5$, subsequently heat treated at 600 °C for 2 h.

an SPS apparatus (SPS-1050, SPS Syntex Inc., Kanagawa, Japan). During the period of heating, a pressure of 30 MPa was applied to the sample. The heating rate was 100 °C/min from room temperature to 800 °C. $Ba_{0.4}Sr_{0.6}TiO_3$ and $CaCu_3Ti_4O_{12}$ end members were also prepared for comparison. All the spark plasma-sintered samples were polished and thermally treated at 600 °C for 2 h in air.

The densities of the sintered samples were measured by the Archimedes method. The crystalline phases of sintered samples were characterized by X-ray diffraction (XRD, D/MAX 2550/PC, Rigaku, Tokyo, Japan) using Cu Kα radiation. The microstructures were observed from the fracture surfaces with field emission scanning electron microscopy (SEM, S-4800, Hitachi, Tokyo, Japan), and element analysis with energy dispersive spectrometer (EDS, EMAX 7593-H, Horiba, Ltd., England). The dielectric properties of the composite ceramics were evaluated from 1 Hz to 10 MHz at temperatures ranging from 135 to 573 K by a broadband dielectric spectrometer (Turnkey Concept 80, Novocontrol Technologies, Germany). Before the dielectric measurement, silver electrodes were pasted on the polished surfaces of the samples.

3. Results and discussion

The sintering behavior of the 0.7BST/0.3CCTO composite ceramics during SPS is shown in Fig. 1. A very small thermal

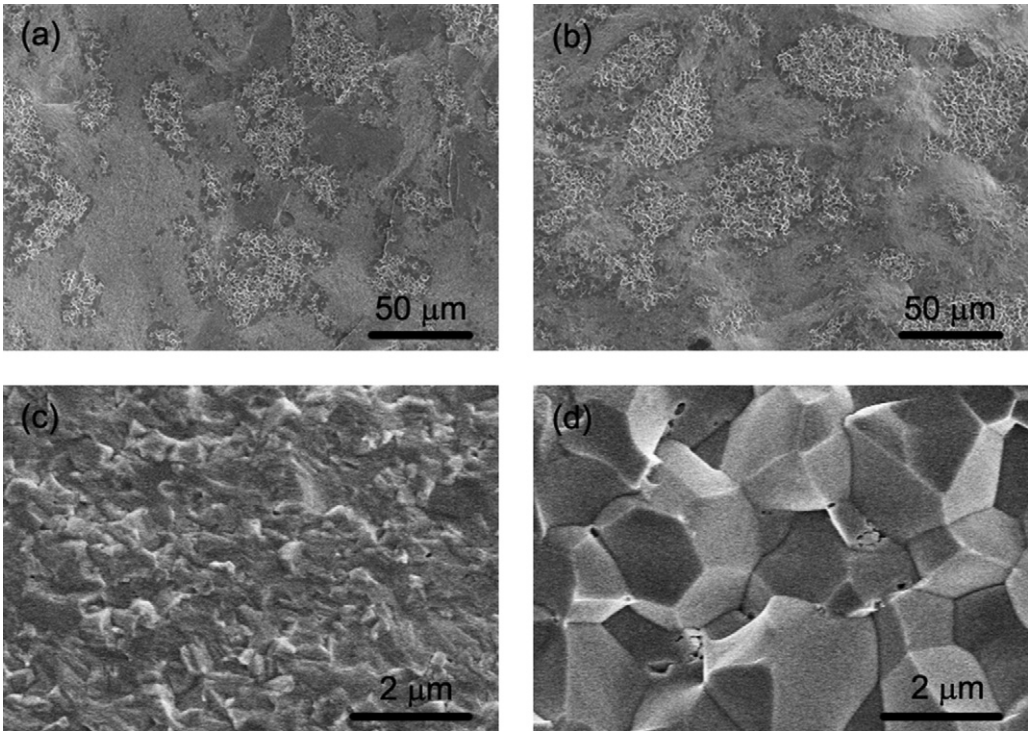

Fig. 3. SEM micrographs of the fracture surfaces for $(1-x)$BST/xCCTO composite ceramics: (a) $x = 0.3$; (b) $x = 0.5$. Enlarged micrographs of (c) large grain regions and (d) small grain regions.

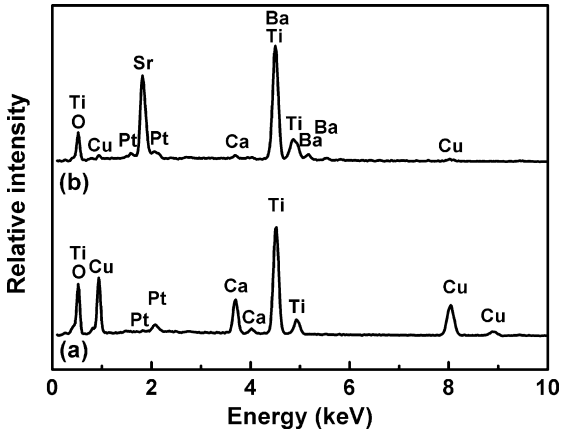

Fig. 4. EDS spectra of BST/CCTO composite ceramics: (a) large grain regions and (d) small grain regions.

expansion was observed when the temperature increased from room temperature to about 680 °C. The shrinkage initiated at about 700 °C, and it increased rapidly as the temperature increased from 700 °C to 800 °C. In order to prevent unexpected interaction between BST and CCTO, no soaking period was employed. The sintering behavior of the 0.5BST/0.5CCTO composite ceramics was similar. Both the relative densities of 0.7BST/0.3CCTO and 0.5BST/0.5CCTO composite ceramics sintered at 800 °C for 0 min by SPS are over 97%, suggesting that a low sintering temperature of 800 °C without soaking period is enough for densification of BST/CCTO composite ceramics by SPS. Although the local temperature of the sample is higher than the temperature measured at the surface of the die, it should be noted that the densification temperature of SPS is about 300 °C lower than that of the conventional solid state sintering. This can be attributed to the microscopic electric discharge between particles and the application of mechanical pressure during SPS. In the initiate period of SPS, the microscopic electrical discharges between particles clean the surfaces of particles from the absorbed species and activate the surface. The cleaned and activated surfaces enhance the diffusion, promote transfer of material, and densify the sample. On the other hand, the application of mechanical pressure aids in removing pores and enhancing the diffusion.

Fig. 2 shows the X-ray diffraction patterns for $(1-x)Ba_{0.4}Sr_{0.6}TiO_3/xCaCu_3Ti_4O_{12}$ ($x = 0.3,\ 0.5$) composite ceramics sintered by SPS. The main phases of all sintered samples are indexed to be cubic perovskite BST phase and CCTO phase without any other detectable crystalline phase, which implies that no obvious chemical reaction occurs between BST and CCTO phase. The diffraction intensities of CCTO phase increases with increasing of x.

The SEM micrographs of fracture surfaces of the BST/CCTO composite ceramics are shown in Fig. 3. It is very clear that two component phases were co-existed and the dense microstructures were observed. The typical micrographs of the large grain regions and the small grains regions are shown in Fig. 3(c) and (d) respectively. Energy dispersive spectroscopy (EDS) spectra of the large grain regions and the small grain regions, as shown in Fig. 4, indicate that the large grains are CCTO and the small grains are BST.

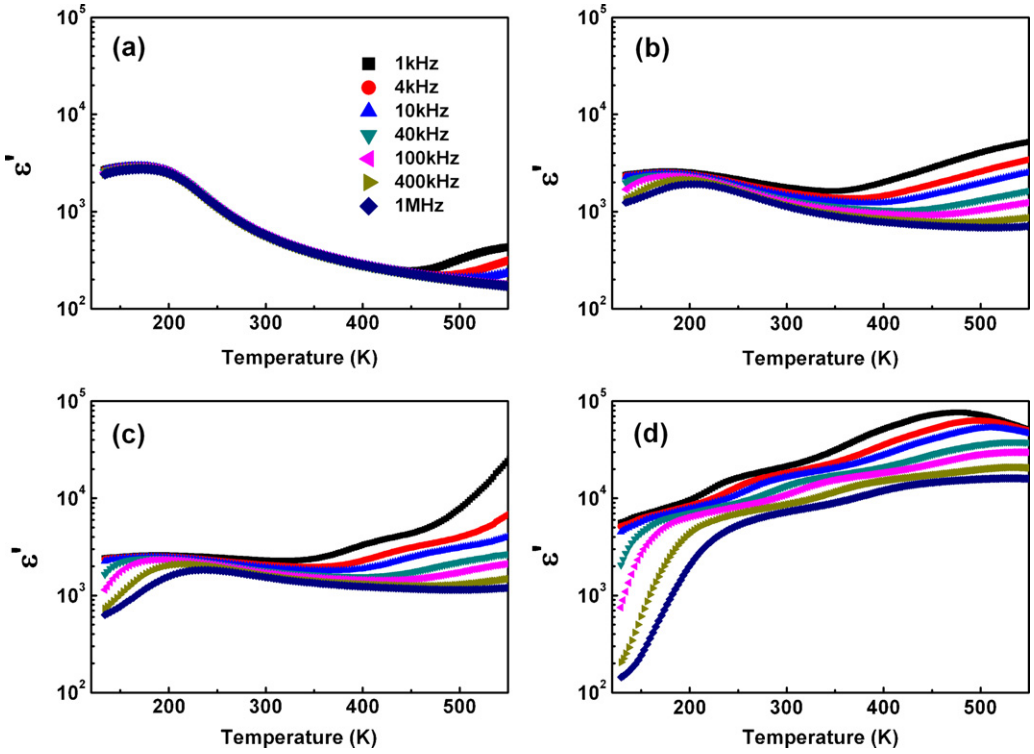

Fig. 5. Temperature dependence of dielectric constant at typical frequencies for (a) BST ceramics; (b) 0.7BST/0.3CCTO composite ceramics; (c) 0.5BST/0.5CCTO composite ceramics; (d) CCTO ceramics.

The temperature dependence of dielectric constant (ε') for CCTO ceramics, BST/CCTO composite ceramics and BST ceramics are shown in Fig. 5. Typical giant dielectric response was observed for CCTO ceramics. The dielectric constant of the CCTO ceramics prepared by SPS at 800 °C for 0 min is lower than that of the CCTO ceramics prepared by the traditional solid state method. This can be attributed to the much smaller grain size of the spark plasma sintered samples. The BST ceramic exhibits typical dielectric response of ferroelectrics with a Curie temperature of about 168 K. The dielectric constant for BST/CCTO ceramics is between those of the BST ceramic and the CCTO ceramics. As the CCTO content increases, the dielectric constant of the BST/CCTO composite ceramics increases.

The dielectric constant and dielectric loss at 100 kHz in the temperature range from 200 to 400 K of CCTO ceramics, BST/CCTO composite ceramics and BST ceramics were compared in Fig. 6. The dielectric constant of the CCTO ceramics increases and the dielectric constant of the BST ceramics decreases with increasing temperature. The BST/CCTO composite ceramics show a much better temperature dependence due to the compensation of the positive temperature coefficient of dielectric constant for the CCTO and the negative temperature coefficient of dielectric constant for the BST. Moreover, compared with the CCTO ceramics, the BST/CCTO composite ceramics have much smaller dielectric losses. The BST/CCTO composite ceramics with high dielectric constant, low dielectric loss and good temperature stability are promising to be utilized for capacitors.

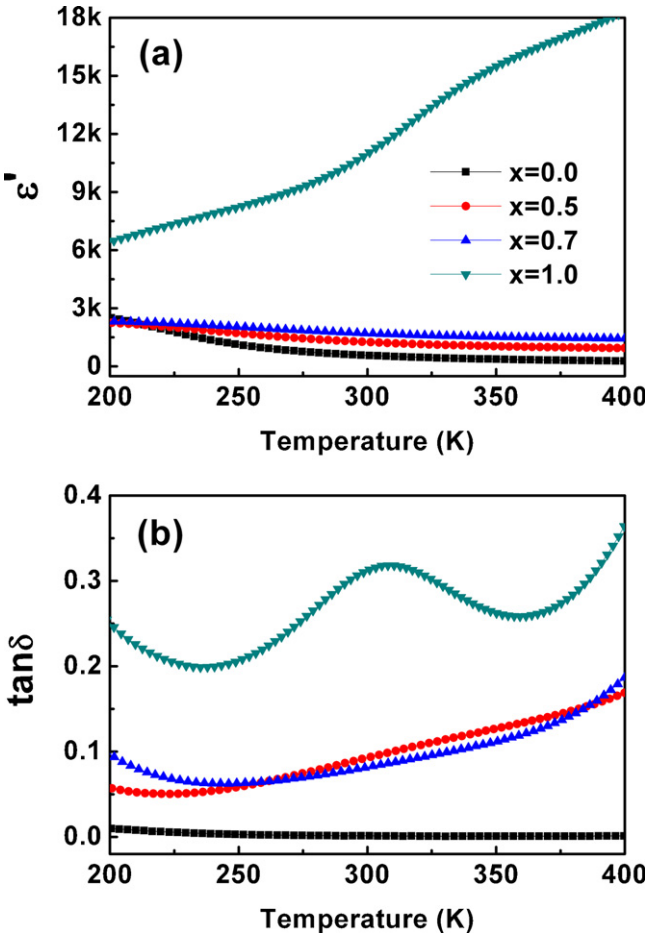

Fig. 6. Temperature dependence of (a) dielectric constant and (b) dielectric loss at 100 kHz for CCTO ceramics, $(1-x)$BST/xCCTO composite ceramics and BST ceramics.

4. Conclusions

$(1-x)Ba_{0.4}Sr_{0.6}TiO_3/xCaCu_3Ti_4O_{12}$ composite ceramics were prepared by spark plasma sintering and their phase constitute, microstructure and dielectric properties were investigated. The dense composite ceramics consisted of BST phase and CCTO phase. The composite ceramics have high dielectric constants between those of the CCTO ceramics and BST ceramics. The dielectric loss of CCTO was decreased and the temperature stability of CCTO was improved by forming the BST/CCTO composite structure. These improvements of dielectric characteristics have great scientific significance for potential application.

Acknowledgements

This work was financially supported by National Science Foundation of China under Grant Nos. 50872121 and 50832005, and National Basic Research Program of China under Grant No. 2009CB623302.

References

[1] M.A. Subramanian, D. Li, N. Duan, B.A. Reisner, A.W. Sleight, High dielectric constant in $ACu_3Ti_4O_{12}$ and $ACu_3Ti_3FeO_{12}$, J. Solid State Chem. 151 (2000) 323–325.
[2] S. Krohns, P. Lunkenheimer, S.G. Ebbinghaus, A. Loidl, Broadband dielectric spectroscopy on single-crystalline and ceramic $CaCu_3Ti_4O_{12}$, Appl. Phys. Lett. 91 (2007) 022910.
[3] A.R. West, T.B. Adams, F.D. Morrison, D.C. Sinclair, Novel high capacitance materials: $BaTiO_3$:La and $CaCu_3Ti_4O_{12}$, J. Eur. Ceram. Soc. 24 (2004) 1439–1448.
[4] L. Ni, X.M. Chen, X.Q. Liu, R.Z. Hou, Microstructure-dependent giant dielectric response in $CaCu_3Ti_4O_{12}$ ceramics, Solid State Commun. 139 (2006) 45–50.
[5] P.B.A. Fechine, A.F.L. Almeida, F.N.A. Freire, M.R.P. Santos, F.M.M. Pereira, R. Jimenez, J. Mendiola, A.S.B. Sombra, Dielectric relaxation of $BaTiO_3$(BTO)–$CaCu_3Ti_4O_{12}$(CCTO) composite screen printed thick films at low temperatures, Mater. Chem. Phys. 96 (2006) 402–408.
[6] G. Yang, Z.X. Yue, X. Li, T. Wang, L.T. Li, Dielectric behavior of $(1-x)BaTiO_3$–$xCaCu_{2.94}Mn_{0.06}Ti_4O_{12}$ composite ceramics, Key Eng. Mater. 368–372 (2008) 62–64.
[7] L. Ramajo, P. Parra, J.A. Varela, M.M. Reboredo, M.A. Ramirez, M.S. Castro, Influence of vanadium on electrical and microstructural properties of $CaCu_3Ti_4O_{12}/CaTiO_3$, J. Alloys Compd. 497 (2010) 349–353.
[8] H. Yu, H. Liu, H. Hao, D. Lou, M. Cao, Dielectric properties of $CaCu_3Ti_4O_{12}$ ceramics modified by $SrTiO_3$, Mater. Lett. 62 (2008) 1353–1355.
[9] M.A. Ramirez, P.R. Bueno, E. Longo, J.A. Varela, Conventional and microwave sintering of $CaCu_3Ti_4O_{12}/CaTiO_3$ ceramic composites: non-ohmic and dielectric properties, J. Phys. D: Appl. Phys. 41 (2008) 152004.
[10] A.D. Hiltonyz, B.W. Rickettsx, Dielectric properties of $Ba_{1-x}Sr_xTiO_3$ ceramics, J. Phys. D: Appl. Phys. 29 (1996) 1321–1325.

[11] P. Liu, J.L. Ma, L. Meng, J. Li, L. Ding, J. Wang, H.W. Zhang, Preparation and dielectric properties of BST–Mg_2TiO_4 composite ceramics, Mater. Chem. Phys. 114 (2009) 624–628.
[12] T. Hu, J. Juuti, H. Jantunen, T. Vilkman, Dielectric properties of BST/polymer composite, J. Eur. Ceram. Soc. 27 (2007) 3997–4001.
[13] Y.J. Wu, N. Uekawa, K. Kakegawa, Sandwiched $BaNd_2Ti_4O_{12}$/$Bi_4Ti_3O_{12}$/$BaNd_2Ti_4O_{12}$ ceramics prepared by spark plasma sintering, Mater. Lett. 57 (2003) 4088–4092.
[14] W.G. Fahrenholtz, E.W. Neuman, H.J. Brown-Shaklee, G.E. Hilmas, Superhard boride–carbide particulate composites, J. Am. Ceram. Soc. 93 (2010) 3580–3583.
[15] Y.J. Wu, S.H. Su, J.P. Cheng, X.M. Chen, Spark plasma sintering of barium zirconate titanate/carbon nanotube composites with colossal dielectric constant and low dielectric loss, J. Am. Ceram. Soc., doi:10.1111/j.1551-2916.2010.04361.x.
[16] N. Ahmad, H. Sueyoshi, Properties of Si_3N_4–TiN composites fabricated by spark plasma sintering by using a mixture of Si_3N_4 and Ti powders, Ceram. Int. 36 (2010) 491–496.
[17] Y. Gao, Y.J. Wu, X.M. Chen, J.P. Cheng, Y.Q. Lin, Y. Ma, Dense YMn_2O_5 ceramics prepared by spark plasma sintering, J. Am. Ceram. Soc. 91 (2008) 3728–3730.
[18] M. Nygren, Z. Shen, On the preparation of bio-, nano- and structural ceramics and composites by spark plasma sintering, Solid State Sci. 5 (2003) 125–131.
[19] Y Ma, X.M. Chen, Y.J. Wu, Y.Q. Lin, Dielectric relaxation and enhanced multiferroic properties in $YMn_{0.8}Fe_{0.2}O_3$ ceramics prepared by in situ spark plasma sintering, Ceram. Int. 36 (2010) 727–731.
[20] T. Takeuchi, M. Tabuchi, H. Kageyama, Y. Suyama, Preparation of dense $BaTiO_3$ ceramics with submicrometer grains by spark plasma sintering, J. Am. Ceram. Soc. 82 (1999) 939–943.
[21] Y.J. Wu, J. Li, X.M. Chen, K. Kakegawa, Densification and microstructures of $PbTiO_3$ ceramics prepared by spark plasma sintering, Mater. Sci. Eng. A 527 (2010) 5157–5160.
[22] Z.A. Munir, U. Anselmi-Tamburini, M. Ohyanagi, The effect of electric field and pressure on the synthesis and consolidation of materials: a review of the spark plasma sintering method, J. Am. Ceram. Soc. 41 (2006) 763–777.
[23] Y. Zhao, L.J. Wang, G.J. Zhang, W. Jiang, L.D. Chen, Preparation and microstructure of a ZrB_2–SiC composite fabricated by the spark plasma sintering-reactive synthesis (SPS-RS) method, J. Am. Ceram. Soc. 90 (2007) 4040–4042.